J Mater Sci (2007) 42:8163–8171
DOI 10.1007/s10853-007-1699-2

# Characterization of starch based nanocomposites

**Ingvild Kvien · Junji Sugiyama · Martin Votrubec · Kristiina Oksman**

Received: 13 December 2006 / Accepted: 15 March 2007 / Published online: 9 June 2007


**Abstract** The goal of this study was to characterize the nanostructure and the properties of starch based nanocomposites with either cellulose nano whiskers (CNW) or layered silicates (LS) (synthetic hectorite) as reinforcements. Modified potato starch was used as matrix with water and sorbitol as plasticizers and with 5 wt.% of either of the reinforcements. Two methods were explored to prepare samples for transmission electron microscopy (TEM) examination; chemical fixation and freeze etching. It was possible to characterize the nanostructure both parallel and perpendicular to the nanocomposite surface by the freeze etching technique. Both nanocomposites showed well-distributed reinforcements in the starch matrix. Dynamic mechanical thermal analysis showed that the storage modulus was significantly improved at elevated temperatures, especially for the layered silicate nanocomposite. Both nanocomposites showed a significant improvement in tensile properties compared to the pure matrix.

I. Kvien · M. Votrubec · K. Oksman
Department of Engineering Design and Materials,
Norwegian University of Science and Technology,
Rich. Birkelandsvei 2b, 7491 Trondheim, Norway

J. Sugiyama
Research Institute for Sustainable Humanosphere (RISH),
Kyoto University, Uji, Kyoto 611-0011, Japan

K. Oksman (✉)
Division of Manufacturing and Design of Wood
and Bionanocomposites, Luleå University of Technology,
931 87 Skelleftea, Sweden
e-mail: kristiina.oksman@ltu.se

## Introduction

Biopolymers are attracting considerable attention as a potential replacement for petroleum based plastics due to an increased consciousness for sustainable development. Biopolymers maintain the carbon dioxide balance after their degradation and are readily biodegradable which will save energy on waste disposal. The limited performance and high cost of these materials are today restricting the competitiveness to traditional thermoplastics. One way to enhance the material properties and to broaden the possible applications for biopolymers is to produce nanocomposites [1].

Starch is a biopolymer which is abundant in nature, is inexpensive and increasingly used as packaging material. It has however poor mechanical properties and a high water affinity. Some studies reported on the preparation of starch based nanocomposites using cellulose nano whiskers (CNW) [2–6] and layered silicates (LS) [7–12]. Starch is hydrophilic and nanocomposites prepared by solution casting and melt blending of unmodified CNW [2–6] and unmodified LS [8, 11] are reported to contain well dispersed reinforcements in contradiction to the use of for example modified LS. There is however only limited insight into the nanostructure of the starch based nanocomposites. For starch containing CNW as reinforcement, no transmission electron microscopy (TEM) work is reported in literature. For these materials scanning electron microscopy (SEM) has exclusively been utilized for structure determination which only gives limited insight into the nanostructure. The resolution of a conventional SEM is limited compared to TEM and there is a need for a more thorough investigation of the structure of CNW/starch nanocomposites. The nanostructure of the layered silicate based nanocomposites is traditionally characterized by a combination of TEM and wide angle X-ray diffraction (WAXD) [13]. However, for starch based

nanocomposites with LS as reinforcement only two studies report on nanostructure characterization using TEM [8, 11]. This is probably because thermoplastic starch has a strong water affinity and thus conventional sample preparation techniques cannot be used to prepare samples for TEM. Preparation of biological samples for TEM examination involves fixation of the specimens, dehydration and infiltration of a resin. Different methods are widely described in literature [14]. Fixation, by cross-linking the starch, will render the starch less hydrophilic [15]. In a previous study on amylose, amylopectin and starch films the samples were fixed in 2% glutaraldehyde [16]. It was however found that the fixation was only effective for the amylose film and both amylopectin and starch films partly dissolved in the preparation step. One way to exclude water from the fixation step for water-soluble specimens is to use vapour fixation [17]. However, different specimens require different fixations and preparative procedures. A major drawback of this method is that the morphology of the sample can be changed upon fixation. Another method for preparation of samples for TEM which also excludes water from the system is the freeze-etching method. By this method the chemical fixation is replaced by freeze fixation and a replica of the freeze-etched surface is prepared. Replication is an old and well-known method for the preparation of specimens for TEM examination [18]. The method is applicable for beam sensitive materials or materials which cannot be prepared by conventional preparation methods, such as water soluble samples. The method is however time consuming and the interpretation of the images is difficult.

The goal of this study was to characterize the nanostructure and the properties of starch based nanocomposites with either CNW or LS as reinforcements. Modified potato starch was used as matrix with water and sorbitol as plasticizers and with 5 wt.% of either of the reinforcements. Two methods were explored to prepare samples for TEM examination; chemical fixation and freeze etching. In addition, the structure of the materials was studied by field emission scanning electron microscope, WAXD and differential scanning calorimetry. The thermal and mechanical performance was analyzed by dynamic mechanical thermal analysis and tensile testing.

## Experimental section

### Materials

#### *Matrix*

Modified normal potato starch, Perlcoat 155, was kindly supplied by Lyckeby Industrial AB (Kristianstad, Sweden). The starch is a hydroxypropylated and oxidized starch, which has good film-forming properties [19]. The degree of substitution with respect to hydroxypropyl groups is 0.11 and with respect to carboxylic acid groups is 0.04 [19]. Normal potato starch contains about 21% amylose and 79% amylopectin. The water content of the starch was 18 wt.% and was used without predrying. D-Sorbitol was used as plasticizer and was supplied by Fluka Chemie GmbH (Buchs, Schweiz).

#### *Reinforcement*

The microcrystalline cellulose (MCC) was kindly supplied by Borregaard Chemcell (Sarpsborg, Norway). It is a powder with particle size of 5–50 μm containing >93% MCC. The LS (synthetic smectite clay/synthetic hectorite) were supplied by Rockwood Additives Limited (Cheshire, U.K.). The tradename is Laponite B and is not organically modified. The bulk density is 0.7–1.3 kg/dm$^3$. The thickness of the disc-shaped sheets is 1 nm and they are 25–40 nm in diameter.

### Processing of nanocomposites

#### *Separation of nanoreinforcement*

The cellulose whiskers were isolated from MCC by acid hydrolysis as described by Bondeson et al. [20]. The LS were dispersed in water at 25 °C for 24 h with stirring. During this time the suspension was sonificated (Hielscher UP 200S, Germany) three times for 5 min. The concentration of both nanoreinforcement suspensions was 0.5 wt.%.

#### *Film preparation*

Starch, sorbitol and CNW or LS (67/28/5) were mixed by first dispersing starch in 100 g of the suspension containing the reinforcement. The gelatinization of starch was performed by stirring this mixture for 30 min at 95 °C. The sorbitol was dissolved in approximately 5 mL water and added to the suspension. The suspension was then poured onto polystyrene petri dishes and the water was evaporated at 70 °C overnight. Films with a thickness of ~0.2 mm were obtained. The films were conditioned for at least three weeks in a desiccator with a saturated solution of magnesium nitrate at 25 °C, which gives a relative humidity of 53% according to ASTM E 104. The films were removed from the desiccator and placed in sealed plastic bags for 24 h and then tested for moisture content and mechanical and dynamic mechanical thermal properties. The final composition and sample codes of the materials are given in Table 1.

**Table 1** Composition of the starch film and the nanocomposites

| Sample code | Dry starch (%) | Sorbitol (%) | Water (%) | Layered silicate (%) | Cellulose whiskers (%) |
|---|---|---|---|---|---|
| S | 62.3 | 31.8 | 5.9 | – | – |
| S-CNW | 58.2 | 29.6 | 6.9 | – | 5.3 |
| S-LS | 57.7 | 29.4 | 7.7 | 5.2 | – |

## Characterization

### *Microscopy*

Optical light microscope (OM) observations were performed using a Leica DMLB. OM was used in order to follow the gelatinization process of starch granules. The magnification used was × 20.

The starch film and nanocomposites were examined in a Hitachi 4300S Field emission scanning electron microscope (FESEM). The accelerating voltage applied was 5 kV. To examine the bulk morphology of the nanocomposites, both fracture surfaces and ultra microtomed surfaces were examined. The surfaces were sputter-coated with platinum before examination.

Transmission electron microscope (TEM) was used to investigate the nanostructure of the materials. The CNW were examined in a Philips CM 30 at 150 kV and the LS and nanocomposites were examined in a Jeol JEM-2000 EX II at 100 kV. To examine the cellulose whiskers and clay particles a droplet of the diluted suspensions was allowed to float on and eventually flow through a copper grid covered with a porous carbon film. The whiskers were stained by floating the grids in a 2 wt.% solution of uranyl acetate for 2 min.

The sample preparation of the nanocomposites for TEM was made using chemical fixation and freeze-etching. For chemical fixation small pieces (30 × 30 mm) of the nanocomposite films were put on a metal net in a glass vessel. 0.8 g *p*-formaldehyde was put in the bottom of the glass vessel. The glass vessel was evacuated and then heated in an oven at 100 °C for 24 h. The samples were then post fixed and stained in OsO4-vapor, rinsed in water and dehydrated in ethanol series. The ethanol was then solvent replaced by propylene oxide followed by resin infiltration and curing with Epon 812.

For the freeze-etching technique the nanocomposite films were cut to rectangular sheets, mounted on holders and then rapidly frozen in liquid propane at –183 °C. The films were freeze-fractured and etched before replicas of the freshly cleaved surface were prepared by carbon coating and shadowing with platinum at 25°. The replicas were gathered onto formvare coated copper grids. Replicas both parallel and perpendicular to the film surface were prepared.

### *Wide angle X-ray diffraction (WAXD)*

The X-ray diffraction patterns of the LS, starch film and the nanocomposites were obtained using a Siemens Diffractometer D5005 (Erlangen, Germany). The samples were exposed for a period of 11 s for each angle of incidence ($\theta$) using a Cu $K\alpha_{1,2}$ X-ray source with a wavelength ($\lambda$) of 1.541 Å. The angle of incidence was varied from ~4° to ~28° by steps of 0.06°. The periodical distances (d) of the main peaks were calculated according to Bragg's equation ($n\lambda = 2d\sin\theta$).

### *Tensile testing*

Tensile testing was carried out using a miniature material tester, Rheometric Scientific MiniMat 2000 (New Jersey, USA), with a 1,000 N load cell at a crosshead speed of 2 mm/min. The materials were removed from the desiccator and placed in sealed plastic bags 24 h prior to testing. The films had a thickness of ~0.2 mm. The samples were prepared by cutting strips from the films with a width of 5 mm. The length between the grips was 15 mm and seven samples were used to characterize each material. The results obtained from the MiniMat 2000 can only be used for comparison, because the strain values are based on the rotational movement of the drive shaft.

### *Dynamic Mechanical Thermal Analysis (DMTA)*

Dynamic mechanical properties of the nanocomposites were measured using a Rheometric Scientific DMTA V (New Jersey, USA) in tensile mode. The measurements were carried out at a constant frequency of 1 Hz, a strain amplitude of 0.05%, a temperature range of –60–180 °C, a heating rate of 3 °C/min and gap distance of 20 mm. The materials were removed from the desiccator and placed in sealed plastic bags 24 h prior to testing to ensure the same humidity level as for tensile testing. The samples were prepared by cutting strips from the films with a width of 5 mm. The films had a thickness of ~0.2 mm. Four samples were used to characterize each material.

### *Differential Scanning Calorimetry (DSC)*

Differential scanning calorimetry (DSC) was performed with Q100 (TA Instruments, New Castle, DE, USA) with a Refrigerated Cooling System (RSC). The samples were placed in a sealed DSC-cell and at least two parallels of

each material were tested. Each sample was heated from –60 °C to +250 °C at a heating rate of 10 °C/min. The glass transition temperature ($T_g$) was taken as the midpoint of the transitions.

## Results and discussion

### Processing and structure

The MCC prior to acid hydrolysis and the layered silicate (synthetic hectorite) before swelling in water are shown in Fig. 1. The particles were ~5–50 μm.

TEM analysis of the suspension after acid hydrolysis of MCC revealed CNW which had a needle-like structure (Fig. 2a). The whiskers were ~5 nm in width and ~200 nm in length as determined in a previous study [21]. The LS had a disc-like structure with diameter 25–40 nm as seen from TEM observation in Fig. 2b. The clay suspension consisted of well-separated clay sheets.

The gelatinization process of starch was followed by light microscopy. Upon gelatinization the starch granules undergoes structural changes. The granules swell and are disrupted as shown in Fig. 3. The amylose leaches out of the swollen granules and the texture becomes gel-like [22].

For processing of the nanocomposites the starch granules were first dispersed in the suspension containing the reinforcement and then gelatinized before the sorbitol was added. This strategy was reported to result in a well-dispersed nanocomposite with LS as reinforcement [10]. The starch matrix was thereby allowed to interact with the reinforcement prior to addition of plasticizer. This procedure was reported to hinder the accumulation of plasticizer in the clay-starch interface [10]. This will be discussed in the section about mechanical properties.

In order to determine if whiskers are well distributed in solutions flow birefringence is often used [23]. Figure 4 shows a picture of the suspension of starch, sorbitol and CNW prior to casting. As can be seen the suspension showed flow birefringence, which indicated a well distribution of the CNW in the starch/sorbitol/water suspension.

After casting, the films were transparent and no visible agglomerates in the nanocomposites could be seen. The appearance of the films is shown in Fig. 5. This indicated well-distributed nanoreinforcement in the starch matrix.

In Fig. 6 fracture surfaces of the films are seen. The surfaces of the starch film and S-LS nanocomposite were very smooth while the S-CNW nanocomposite was rougher. Small white particles were detectable in the S-CNW nanocomposite and it is uncertain whether this was due to small clusters of agglomerated cellulose whiskers emerging from the matrix, the matrix itself evolving due to the influence by the electron beam or contamination during sample preparation. There were no big agglomerates of cellulose whiskers detectable which indicates a homogenous distribution of the cellulose whiskers in the matrix. In the S-LS nanocomposite the surface seemed smooth and there were no layered silicate sheets detectable. This can be due to lack of resolution, the coating of the platinum particles or because of well-distributed clay sheets. No agglomerates of LS were detectable. Ultramicrotomed surfaces of the samples were also investigated. The appearance of these surfaces resembled those of the fractured surfaces as seen from the pictures in Fig. 7.

For TEM analysis of the nanocomposites it was found that the sample preparation was challenging. After chemical fixation by *p*-formaldehyde vapor, the films appeared less brittle and more rubber-like than before treatment. It thus seemed that the treatment was effective in cross-linking the starch. However, after the dehydration steps and embedding in resin, it was still not possible to obtain ultra thin sections of the nanocomposites. The sections instantly disappeared from the water surface after sectioning and it was therefore not possible to analyze the samples in TEM by this method. It was however found that it was possible to prepare starch based nanocomposite for TEM analysis by using the freeze-fracture technique. This technique allowed examination of the bulk structure both parallel and perpendicular to the film surface. In Fig. 8 and nine replicas of the S-CNW and S-LS nanocomposites, respectively, are shown. Both reinforcements were well distributed in the starch matrix, although they appeared denser in

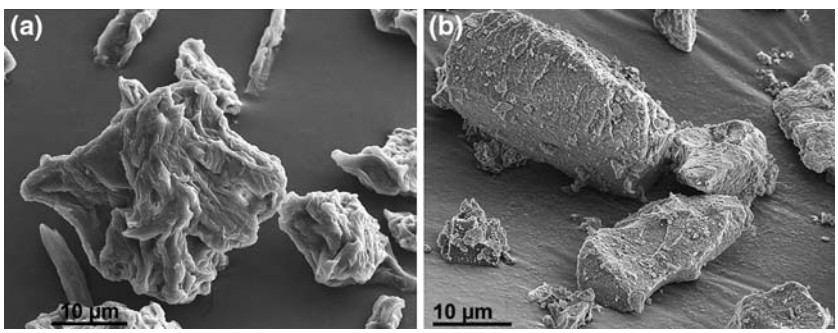


**Fig. 1** The structure of (**a**) MCC and (**b**) layered silicate particles prior to separation

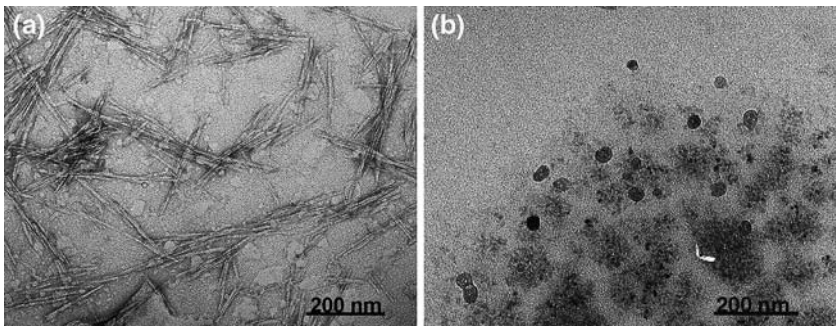


**Fig. 2** (**a**) Bright field TEM image of stained cellulose whiskers and (**b**) layered silicate sheets after mixing in water for 24 h

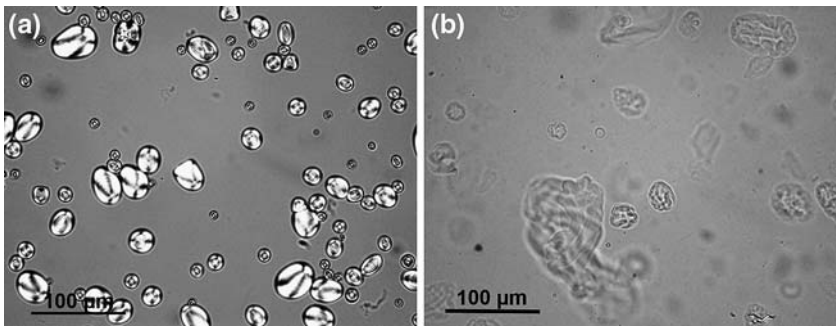


**Fig. 3** Starch granules seen in polarized light at (**a**) room temperature and (**b**) at 95 °C after 30 min

some areas. In Fig. 8a the presence of cellulose nano whiskers was observed as a fibrillated texture in the starch matrix. This texture was not observed in the S-LS nanocomposite. These observations indicate that the CNW were removed by the knife during cutting and therefore small holes were formed from the whisker pullouts. The texture may also be due to underlying structure of cellulose whiskers. In other areas the CNW seemed to protrude from the surface, as observed for the cross section replica in Fig. 8b. There was a tendency for the CNWs to arrange parallel to the film surface. It is important to note that the replica is only a copy of the cut surface and therefore has limited access to the bulk structure. In this case only the top of the whiskers could be observed. Similar trend was seen for the S-LS nanocomposite. The silicate sheets were observed as disc-like structures with the same size as observed in the TEM image of the dried layered silicate suspension in Fig. 2b. In the cross section replica (Fig. 9b) only a part of the sheets was observed, which suggest a

**Fig. 4** A suspension of starch, sorbitol and cellulose nano whiskers in water showing flow birefringence when observed through crossed polarizers

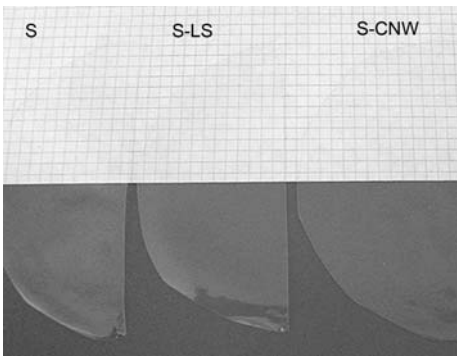


**Fig. 5** Transparent films of starch, S-LS and S-CNW nanocomposites

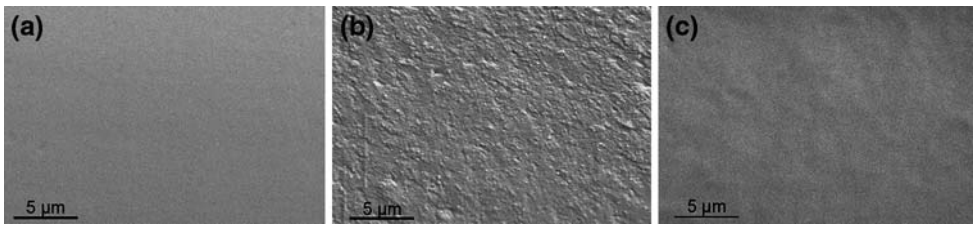


**Fig. 6** FESEM pictures of fracture surfaces of (**a**) starch (**b**) S-CNW and (**c**) S-LS nanocomposites

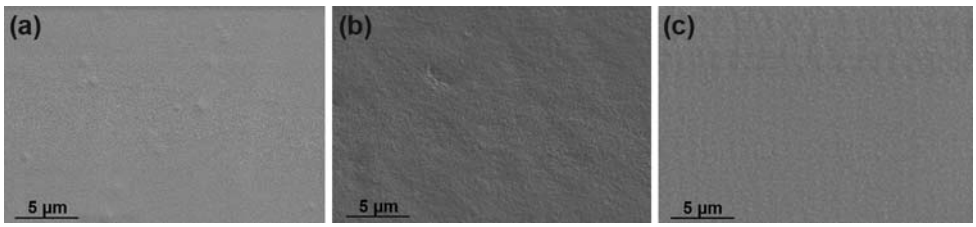


**Fig. 7** FESEM pictures of ultramicrotomed surfaces of (**a**) starch (**b**) S-CNW and (**c**) S-LS nanocomposites

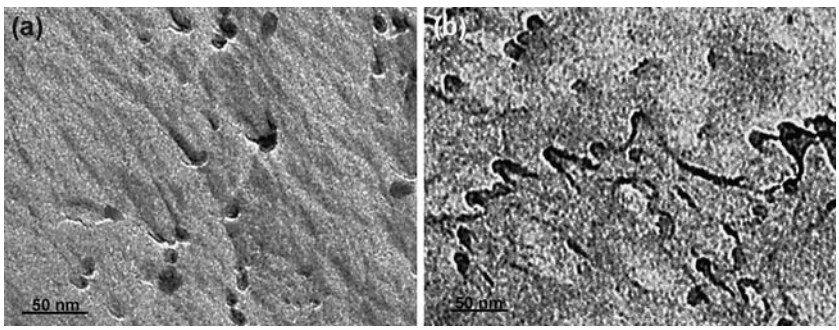


**Fig. 8** TEM images of replica of S-CNW nanocomposite (**a**) parallel and (**b**) perpendicular to the film surface

tendency for the LS to arrange parallel to the film surface. From the cross section replica it seemed that the S-LS nanocomposite had an exfoliated structure. In areas where the presence of the LS was denser the distance between the sheets was difficult to determine, and the nanocomposite might locally have an intercalated structure.

Wide angle X-ray diffractograms of the samples are shown in Fig. 10. Both the starch film and the nanocomposites showed an amorphous behavior. No diffraction peak was observed, but rather a broad hump located at around $2\theta = 20°$. The diffractogram of the pure LS powder did not show a well-defined 001 peak. The Laponite B particles are relatively small and therefore have a random orientation when prepared as pressed powder which can prevent the 001 peak from showing up very well. However, in the diffractogram of the freeze dried LS suspension the 001 peak appeared at around $2\theta = 7°$. The layers were now more oriented in the 001 plane. This corresponds to a distance between the layers of 1.24 nm according to Braggs law. In the diffractogram of the S-LS nanocomposite, no signal from the 001 peak was observed which indicates that the distance between the silicate sheets was larger than detectable by the low angle limit. The starch molecules or sorbitol and water were thus probably able to penetrate between the silicate sheets and thereby creating an exfoliated structure. It is worth noting that there was

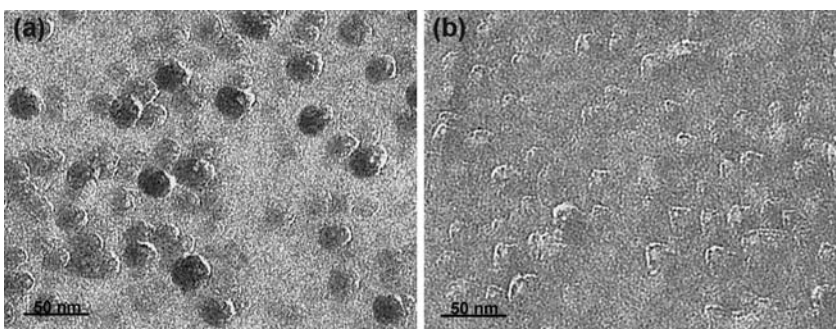


**Fig. 9** TEM images of replica of S-LS nanocomposite (**a**) parallel and (**b**) perpendicular to the film surface

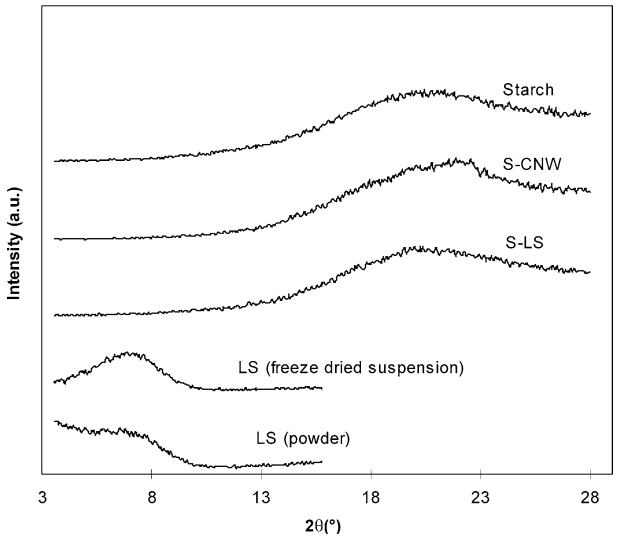


**Fig 10** Wide angle X-ray diffraction of the starch, layered silicate and nanocomposites

only 5 wt.% LS in the nanocomposite and therefore the X-ray diffraction analysis may fail in detecting the crystalline structure of the reinforcement in the polymer. However, the TEM observations showed that the silicate sheets were arranged parallel to the film surface and was therefore expected to give a detectable signal if the distance between the sheets had been in the range detectable by the analysis.

## Mechanical and thermal properties

### *Tensile testing*

The mechanical properties of the starch film and the nanocomposites are given in Table 2. Both nanocomposites showed an improvement in tensile modulus, yield strength and elongation at break compared to the pure matrix. The CNW and LS nanocomposites showed an improved tensile modulus compared to the neat material by 90 MPa (24%) and 100 MPa (27%), respectively. This is a significant improvement compared to other studies on starch nanocomposites with 5 wt.% reinforcement [2, 3, 6, 10, 11]. The tensile strength was only slightly improved, a result which is also reported in earlier studies. In this study the starch matrix as received contained propyl groups which might contribute to restricted interaction with the highly hydrophilic reinforcements.

Unexpectedly, the elongation at break was increased for both nanocomposites compared to the pure matrix. This behavior has not earlier been reported for CNW based starch nanocomposites, but has been reported for LS based nanocomposites [10, 11]. Pandey [10] explained that the increased elongation at break was due to the processing of

**Table 2** Tensile properties of the starch film and the nanocomposites

| Materials | Tensile modulus (MPa) | Yield strength (MPa) | Elongation at break (%) |
|---|---|---|---|
| Starch | 370 ± 35 | 11.3 ± 1.0 | 25 ± 11 |
| S-CNW | 460 ± 10 | 13.7 ± 1.3 | 32 ± 10 |
| S-LS | 470 ± 45 | 12.5 ± 1.3 | 31 ± 12 |

their materials in which the plasticizer was mixed after starch diffusion inside the gallery and would therefore migrate throughout the system and retaining the plasticizer efficiency. The gelatinization of starch together with cellulose whiskers prior to addition of plasticizer has not been reported earlier and might explain the increased elongation at break in this study. This indicates that the sorbitol was not present on the surface of the reinforcement as reported earlier when glycerol was used as plastizicer [6], but was distributed throughout the material. In addition, the moisture content was slightly higher in the nanocomposites, and this may also be the reason for the increased elongation at break. Typical stress–strain curves for the materials are given in Fig. 11.

### *Dynamic mechanical thermal analysis*

The storage modulus of the starch film and nanocomposites as a function of temperature is given in logarithmic scale in Fig. 12a. In Table 3 the calculated storage modulus at 25 °C and 60 °C is given. The CNW nanocomposite showed an improved storage modulus above room temperature compared to the starch film. The S-LS nanocomposite showed an improved storage modulus over the entire temperature span. The improvement in storage modulus was more pronounced at elevated temperatures for both nanocomposites where the molec-

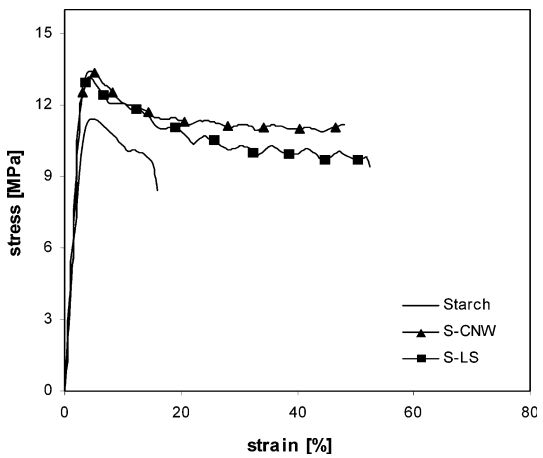


**Fig. 11** Stress–strain curves of starch film, S-CNW and S-LS nanocomposites

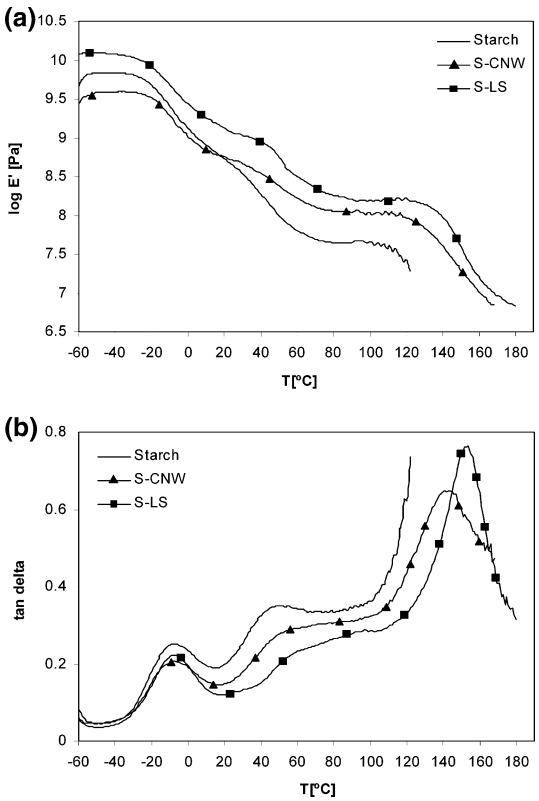


**Fig. 12** (**a**) Storage modulus and (**b**) tan delta curves of the starch and nanocomposites

ular relaxation for the starch matrix occurs. The starch film showed a rather large standard deviation in the storage modulus up to room temperature. This might be due to difficulties in accurate measurement of the soft starch matrix prior to testing and thickness variations throughout the sample. At room temperature (25 °C) the CNW and the LS nanocomposites showed an improvement of 132 MPa (36%) and 650 MPa (176%), respectively, compared to the pure starch film. At 60 °C the improvement was even more; a 113 MPa (164%) and 217 MPa (314%) increase of the storage modulus for the CNW and the LS nanocomposite, respectively, compared to the pure starch film. This is a significant improvement compared to earlier dynamic mechanical data with similar reinforcement content [2, 6, 11]. It was calculated

**Table 3** Storage modulus of the materials from DMTA analysis 25 °C and 60 °C

| Materials | Storage modulus at 25 °C (MPa) | Storage modulus at 60 °C(MPa) |
|---|---|---|
| Starch | 370 ± 97 | 69 ± 7 |
| S-CNW | 502 ± 10 | 182 ± 20 |
| S-LS | 1,020 ± 20 | 286 ± 40 |

that the theoretical available surface area of the layered silicate sheets was 4 times higher than the available surface area of the CNW. This might explain the more efficient reinforcing effect of the clay sheets. The tensile modulus of the LS nanocomposite did not seem to correlate with the storage modulus measured from dynamic mechanical data. This might be due to the fact that dynamic mechanical measurements involve weak stresses. Higher stresses are utilized in tensile testing and thus, the interaction between the reinforcement and matrix may be destroyed in this case [6].

In Fig. 12b the tan delta is shown for the same temperature range, showing three different relaxation peaks. The first peak was seen at –10° and it is suggested to be caused by the relaxation of sorbitol [24]. The peaks were slightly lower for the nanocomposites, but these materials also contained less sorbitol. The position of the peaks was not altered for the three materials. However, the next transition which occurred at 50 °C for the starch material and is attributed to the relaxation of the starch [6, 24, 25] was shifted to higher temperatures for the nanocomposites. This transition was not well-defined and probably more transitions occurred in this area. According to Butler and Cameron [25] polysaccharides show relaxation processes in three temperature ranges. In the glassy state the relaxation is attributed to secondary relaxations such as rotation of the methylol group. At higher temperatures the relaxation is attributed to the glass-rubber transition and motion of bound water. The last relaxation is attributed to water loss and chain stiffening. The peaks were not well-defined and therefore the shift in the tan delta peak was difficult to estimate, but the peaks were lower and broader than for the pure matrix. Thus, the starch chains were altered by the introduction of nanoreinforcement and therefore the relaxation of starch was done in a higher and broader temperature range. This indicates interaction between the starch and reinforcement and that the nanoreinforcement was well dispersed in the starch matrix. This also strengthens the conclusion from the tensile testing that the plasticizer was not present in the starch/reinforcements interfacial zone. It was not possible to complete the measurement of the starch film during the third transition due to extensive drop in mechanical properties. The third transition was probably due to melting of crystals in the starch matrix. This was unexpected since the X-ray analysis concluded all materials to be amorphous. However, the DMTA measurements were done several weeks after the X-ray analysis and therefore the crystal formation may be due to aging of starch through crystallization. This is known as retrogradation and is caused by reassociation during storage of amorphous gelatinized starch into a more ordered state [26].

**Table 4** DSC results of the starch film and the nanocomposites

| Sample | Tg sorbitol (°C) | Tg starch (°C) | Tm (°C) |
|---|---|---|---|
| Starch | –17 | 55 | 134 |
| S-CNW | –12 | 70 | 154 |
| S-LS | –11 | 79 | 160 |

*Differential scanning calorimetry (DSC)*

DSC was performed to confirm the thermal transitions and to investigate further the third transition observed in DMTA analysis. The results from DSC are given in Table 4. The results are only approximately values since the transitions were taking place over a broad temperature range and were therefore difficult to estimate accurately. The results correlated quite well with DMTA analysis. A melting point was found for all three materials. Interestingly, the melting point of the two nanocomposites was significantly shifted to higher temperatures. It thus seemed that the presence of the nanoreinforcement in the starch matrix influenced the size and amount of crystals formed in the starch matrix.

## Conclusions

The goal of this study was to characterize the nanostructure and the properties of starch based nanocomposites with two different nanoreinforcements, CNW or LS. Modified potato starch was used as matrix with water and sorbitol as plasticizers and with 5 wt.% nanoreinforcement content.

Two methods were explored to prepare the samples for TEM examination; chemical fixation and freeze etching. It was found that the chemical fixation with *p*-formaldehyde vapour treatment of starch was not sufficient to enable ultrathin sectioning of the nanocomposite films. It was however shown that it was possible to characterize the nanostructure both parallel and perpendicular to the nanocomposite surface by preparation of replicas prior to TEM examination. Both reinforcements were well distributed in the starch matrix, although some agglomerations were found in some areas.

From X-ray diffraction analysis it was found that all the prepared materials were amorphous. X-ray analysis showed well distributed silicate sheets in the starch matrix, as seen by TEM observations.

Both nanocomposites showed an improvement in tensile modulus, yield strength and elongation at break compared to the pure matrix. The CNW and LS nanocomposites showed an improved tensile modulus compared to the neat material by 90 MPa (24%) and 100 MPa (27%), respectively. The order of the addition of plasticizer was concluded to influence the elongation at break for both nanocomposites. It was found that the plasticizer was not present in the starch/reinforcements interfacial zone. The dynamic mechanical thermal analysis showed that at room temperature the storage modulus of CNW and LS nanocomposites were improved by 74 MPa (17%) and 705 MPa (162%), respectively, compared to the pure starch film. At 60 °C the improvement was 102.7 MPa (160%) and 250 MPa (388%) for the CNW and the LS nanocomposite compared to the pure starch film.

**Acknowledgements** Borregaard AS (Sarpsborg, Norway) is acknowledged for the MCC and Lyckeby Industrial AB (Kristianstad, Sweden) is acknowledged for the starch. The Norwegian Research Council under the NANOMAT program is acknowledged for financial support of this work. The Laboratory of Active Biobased Materials at RISH, Kyoto University, Japan, and in particular Professor Hiroyuki Yano and Shin-ichirou Iwamoto are acknowledged for providing equipment and help with the formaldehyde treatment of starch. A special thanks to Chiori Itoh and Dr. Thi Thi Nge at The Laboratory of Biomass Morphogenesis and Information at the Research Institute for Sustainable Humanosphere (RISH), Kyoto University, Japan, for all the help with sample preparation and TEM observations.

## References

1. Mohanty AK, Drzal LT, Misra M (2003) Polym Mater Sci Eng 88:60
2. Lu Y, Weng L, Cao X (2006) Carbohydr Polym 63:198
3. Lu Y, Weng L, Cao X (2005) Macromol Biosci 5:1101
4. Mathew AP, Dufresne A (2002) Biomacromolecules 3:609
5. Anglès MN, Dufresne A (2000) Macromolecules 33:8344
6. Anglès MN, Dufresne A (2001) Macromolecules 34:2921
7. Liao H-T, Wu C-S (2005) J Appl Polym Sci 97:397
8. Chen B, Evans JRG (2005) Carbohydr Polym 61:455
9. Chen M, Chen B, Evans JRG (2005) Nanotechnology 16:2334
10. Pandey JK, Singh RP (2005) Starch/Stärke 57:8
11. Park H-M, Lee W-K, Park C-Y, Cho W-J, Ha C-SJ (2003) J Mater Sci 38:909, DOI: 10.1023/A:1022308705231
12. Wilhelm H-M, Sierakowski M-R, Souza GP, Wypych F (2003) Carbohydr Polym 52:101
13. Ray SS, Okamoto M (2003) Progr Polym Sci 28:1539
14. Gluert AM (1975) Practical methods in electron microscopy. North Holland Publishing Company
15. Zhu Z, Cao S (2004) Text Res J 74(3):253
16. Rindlav-Westling Å, Stading M, Gatenholm P (2002) Biomacromolecules 3:84
17. Grote M (1992) Microsc Res Tech 21:242
18. Sawyer LC, Grubb DT (1994) Polymer microscopy. Chapman and Hall, London
19. Jansson A, Järnström L (2005) Cellulose 12:23
20. Bondeson D, Mathew A, Oksman K (2006) Cellulose 13(2):171
21. Kvien I, Tanem BS, Oksman K (2005) Biomacromolecules 6(6):3160
22. Hermansson AM, Svegmark K (1996) Trends Food Sci Technol 7:345
23. Heux L, Chauve G, Bonini C (2000) Langmuir 16:8210
24. Gaudin S, Lourdin D, Forssell PM, Colonna P (2000) Carbohydr Polym 43:33
25. Butler MF, Cameron RE (2000) Polymer 41:2249
26. Mathew AP, Dufresne A (2002) Biomacromolecules 3:1101